JCB Article

Intraflagellar transport balances continuous turnover of outer doublet microtubules: implications for flagellar length control

Wallace F. Marshall and Joel L. Rosenbaum

Department of Molecular, Cellular, and Developmental Biology, Yale University, New Haven, CT 06520

A central question in cell biology is how cells determine the size of their organelles. Flagellar length control is a convenient system for studying organelle size regulation. Mechanistic models proposed for flagellar length regulation have been constrained by the assumption that flagella are static structures once they are assembled. However, recent work has shown that flagella are dynamic and are constantly turning over. We have determined that this turnover occurs at the flagellar tips, and that the assembly portion of the turnover is mediated by intraflagellar transport (IFT). Blocking IFT inhibits the incorporation of tubulin at the flagellar tips and causes the flagella to resorb. These results lead to a simple steady-state model for flagellar length regulation by which a balance of assembly and disassembly can effectively regulate flagellar length.

Introduction

A fundamental question in cell biology that remains unanswered is how cells regulate the size of their organelles. Does size regulation imply the existence of "size-measuring machinery?" Answering such a question experimentally is challenging, in part because of the difficulty in measuring the size of an organelle that has a three-dimensional shape. However, the flagellum or cilium has a one-dimensional structure, and its size can be determined simply by measuring its length.

One can easily measure flagellar length and screen for length mutations in the biflagellate alga *Chlamydomonas*, and this has enabled the isolation of several types of mutants with abnormal length flagella. Among these are the long flagella (*lf*)* (McVittie, 1972; Jarvik et al., 1976; Barsel et al., 1988; Asleson and Lefebvre, 1998), short flagella (*shf*) (Jarvik et al., 1984; Kuchka and Jarvik, 1987), and flagellar assembly (*fla*)–defective mutants (Huang et al., 1977). It is not yet known how any of these genes act to regulate flagellar length.

To understand how flagellar length is regulated, it is important to determine whether flagella are dynamic structures, i.e., are the components of the flagellum turning over? One might think this is an unreasonable question, as all parts of a living cell are turning over to one extent or another. However, historically, ciliary and flagellar microtubules have been regarded as "stable" and rather "static" structures (Behnke and Forer, 1967; Tilney and Gibbins, 1968), not changing in length in the presence of microtubule depolymerizing drugs such as colchicine and nocodazole, and maintaining their length in the cold. However, detailed radioactive pulse labeling studies (Gorovsky et al., 1970; Stephens, 1992, 1997, 2000; Song and Dentler, 2001) have shown quite clearly that all parts of the flagellum are turning over. More recently, it has been shown in *Caenorhabditis elegans* that genes required for the assembly of sensory cilia during embryogenesis continue to be expressed in the adult after cilia are fully assembled, and that they are required for sensory cilia maintenance (Fujiwara et al., 1999). Therefore, there is no question that the flagellar axonemal microtubules and their associated structures are dynamic.

The phenomenon of intraflagellar transport (IFT) provides further evidence that flagella are dynamic structures. IFT is a motile process within flagella in which large protein complexes move from one end of the flagellum to the other (Kozminski et al., 1993b, 1995). Anterograde movement of these particles to the plus end of the flagellum is driven by a heterotrimeric kinesin-II, one motor subunit of which is encoded by the flagellar assembly (*FLA*)*10* gene in *Chlamydomonas*. Temperature-sensitive *fla10* mutants (Huang et

Address correspondence to Wallace Marshall, KBT310 MCDB Dept., Yale University, New Haven, CT 06520-8103. Tel.: (203) 432-3473. Fax: (203) 432-6161. E-mail: wallace.marshall@yale.edu

*Abbreviations used in this paper: *fla*, flagellar assembly; HA, hemaglutinin; IFT, intraflagellar transport; *lf*, long flagella; *shf*, short flagella.

Key words: flagella; tubulin; *Chlamydomonas*; kinesin; intraflagellar transport

al., 1977) prevent flagellar regeneration by arresting anterograde IFT at the nonpermissive temperature (Kozminski et al., 1995). IFT is required to transport inner dynein arms (Piperno et al., 1996) and presumably other axonemal subunits to the end of the growing flagellum, which is the site of new flagellar protein assembly during regeneration (Rosenbaum and Child, 1967; Johnson and Rosenbaum, 1992).

Remarkably, IFT continues to be required even after flagellar assembly is completed. When *fla10* mutants with intact flagella are shifted to the nonpermissive temperature, IFT stops (Kozminski et al., 1995) and the flagella begin to shorten and eventually disappear (Huang et al., 1977). This shortening would not occur if flagella were static structures. It suggests that flagella require a constant input of subunits to balance the loss during turnover, and emphasizes the dynamic nature of the flagellar axoneme. These turnover results raise several interesting questions, the first of which is, where along the flagellar length does the turnover occur? How much of the flagellar axoneme is turning over? Is the rate and extent of turnover sufficient to account for the rate of the complete flagellar resorption that occurs in *fla10* mutants at the nonpermissive temperature when IFT is inhibited? Finally, one might also ask how such a turnover process fits in with mechanisms for flagellar length control.

In order to determine the cytological localization and spatial extent of turnover, we have developed an assay to visualize turnover of tubulin in *Chlamydomonas* flagella. Our results show that tubulin assembles and disassembles continuously at the distal end of the flagella, indicating that flagella are dynamic structures. We have also found that IFT is required for the steady-state assembly of outer doublet microtubules that occurs during turnover. On the other hand, the continuous disassembly of outer doublet microtubules was found to continue in the absence of IFT. These results suggested that length regulation may involve a balance between continuous assembly of tubulin at the tip, mediated by IFT, balanced by continuous disassembly. Consistent with this idea, we find that partial reduction in IFT leads to an *shf* phenotype, and conversely we find that an *lf* mutant shows a decreased rate of turnover.

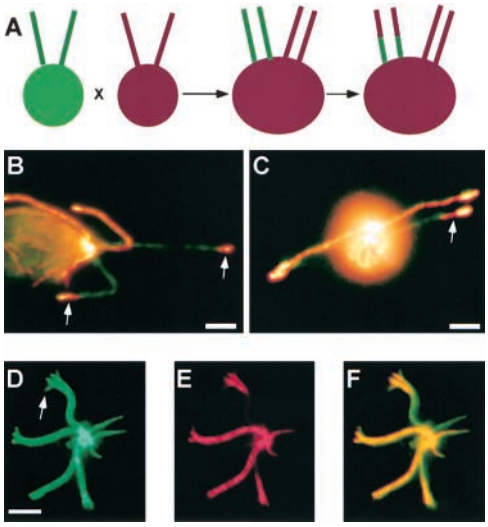

Figure 1. **Visualizing flagellar microtubule dynamics.** (A) Experimental strategy. Cells expressing HA-tubulin are mated with nonexpressing cells to create a quadriflagellated dikaryon in which two flagella contain HA-tubulin and two do not. Cells are fixed at successive timepoints after mating, and stained with antibodies recognizing HA-tubulin, to detect incorporation of tagged tubulin into the previously unlabeled flagella. (B and C) Typical dikaryon images. Cell fixed 90 min after mating. (Green) FITC immunofluorescence with antibodies to *Fla10* kinesin, used as a marker for flagella and basal bodies. (Red) Texas red immunofluorescence with antibodies recognizing the HA epitope–tagged tubulin. Yellow results from overlap of HA-tubulin staining with *Fla10* kinesin staining, indicating incorporation of tagged tubulin into flagella. Two flagella (originally belonging to the tagged tubulin expressing cell) are fully labeled and two are partially labeled (arrows), indicating incorporation of tagged tubulin following mating. (D–F) Flagella splayed open with detergent plus ATP following mating of HA-tagged tubulin expressing and nonexpressing cells. (D) Splayed flagella detected by FITC immunofluorescence using antibodies against tubulin. Central pair microtubules (arrow) have extruded and are clearly separated from the main mass of outer doublets. (E) Texas red immunofluorescence using antibodies to HA epitope-tagged tubulin. Tagged tubulin clearly has incorporated into the distal end of the outer doublets, and possible also the splayed-out central pair microtubules. (F) Overlay image showing that majority of incorporation is in the outer doublet microtubules. Bars: (B and C) 2 μm; (D–F) 3 μm.

Results

Visualizing flagellar microtubule turnover

A method was developed to visualize flagellar microtubule turnover in situ in *Chlamydomonas*. As illustrated in Fig. 1 A, cells expressing hemaglutinin (HA) epitope–tagged α-tubulin were mated to wild-type cells that lacked the tagged tubulin construct. Upon mating, the biflagellate *Chlamydomonas* gametic cells fused to form a quadriflagellate dikaryon. At this point, only two of the four flagella contained HA-tagged tubulin. If flagellar tubulin turns over, HA-tubulin should begin to incorporate into the other two unlabeled flagella of the cell that did not initially contain tagged tubulin. As indicated by the arrows in Fig. 1, B and C, tagged tubulin was indeed found to incorporate into the distal regions of these flagella.

To localize this incorporation more precisely, cells were washed with detergent to remove the flagellar membrane and then treated with ATP, allowing the dynein arms to rupture the flagella. Under these conditions, the set of nine outer doublets splits into two groups and the central pair microtubules splay out through the gaps (Johnson, 1998). As seen in Fig. 1, D–F, when partially labeled flagella in the course of these dikaryon experiments were splayed in this way, HA-tubulin had clearly incorporated into the outer doublets.

Having demonstrated that tubulin incorporates into the outer doublets at the distal end, we next measured the spatial extent of this incorporation over time. Dikaryons were fixed at 20-min intervals after mating. At each time point, the average length of the distal labeled region and the proximal unlabeled region were measured, with results plotted in Fig. 2. As time elapsed after cell fusion, tagged tubulin incorporation could be seen over an increasingly larger distal region of the flagella. During this time, the flagella were not growing. Flagella shorten gradually following mating, as seen in Fig. 2. In spite of this, we are still able to measure the rates

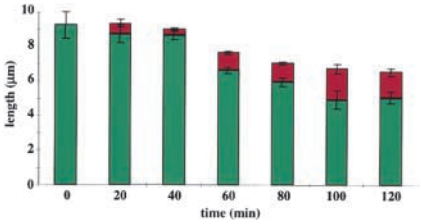

Figure 2. **Measuring turnover based on spatial distribution of incorporated HA-tagged tubulin versus time.** Each bar represents average labeling of flagella at a given time point after cell fusion. Red segment gives average length of labeled portion, green segment gives average length of unlabeled portion. Over time, HA-tagged tubulin incorporates over an increasingly large distal portion of the flagellum. At the same time, flagella are not growing but are in fact shortening as a consequence of the mating developmental pathway. Therefore, incorporation does not simply reflect residual flagellar growth, but must entail turnover of tubulin already present in the flagellum. Average number of flagella measured per time point was 27. Error bars in all graphs represent standard error of the mean.

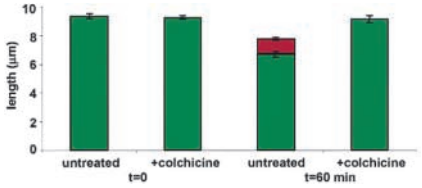

Figure 3. **Colchicine blocks flagellar tubulin turnover in wild-type cells.** Compared to untreated cells, in cells treated with 3 mg/ml colchicine, a concentration that totally blocks flagellar regeneration, no assembly of HA-tubulin was observed at the distal ends of the flagella, confirming that the assembly observed in untreated cells represents bona fide microtubule polymerization. Colchicine also completely blocked disassembly of the outer doublets, thereby shutting down turnover. Average number of measurement per graph entry is 28.

of assembly and disassembly by measuring the changes in the lengths of the labeled and unlabeled segments. However, we note that the apparent rates of assembly and disassembly measured here apply strictly to mated cells, and are likely to be slightly different in vegetative cells. The time course of the experiment was limited to ~120 min because after longer time intervals, all four flagella rapidly and synchronously resorb in preparation for meiosis. Consequently, we were not able to observe these cells long enough to see complete labeling of the flagella. Nevertheless, after 120 min, in some cases as much as a third of the flagellum was found to incorporate tagged tubulin. Fig. 2 shows that the labeled region at the distal end of the flagellum grew at the expense of the unlabeled region, causing the unlabeled proximal region to appear to shorten throughout the course of the experiment. The continuous addition of new tubulin in the absence of growth indicated that during the course of the experiment, old unlabeled tubulin subunits were continuously removed in order to accommodate the new tubulin assembly, i.e., turnover was occurring.

Colchicine blocks both tubulin addition and removal

Colchicine at a concentration sufficient to prevent flagellar regeneration does not cause flagellar shortening (Behnke and Forer, 1967; Tilney and Gibbins, 1968; Rosenbaum et al., 1969), and this is frequently taken as evidence that flagellar microtubules are not turning over (see, for example, Jensen et al., 1987; Tilney et al., 2000). The dikaryon assay of Fig. 1 was repeated in the presence of colchicine at a concentration of 3 mg/ml, a concentration sufficient to completely block flagellar regeneration following deflagellation. As plotted in Fig. 3, colchicine did indeed completely block incorporation of tagged tubulin into flagella, confirming that the incorporation of tubulin into the outer doublets seen in Fig. 1 represents bona fide microtubule polymerization. In addition, colchicine also blocked the removal of unlabeled tubulin that we had observed in untreated cells, as indicated by the fact that the unlabeled proximal segment did not become shorter. Therefore, colchicine seems to arrest all microtubule dynamics within the flagellum, and the fact that colchicine does not cause flagella to shorten is misleading and cannot be taken as evidence against microtubule turnover. We do not know how colchicine blocks turnover and disassembly, but one possibility is that colchicine-tubulin dimers might cap the plus ends of the outer doublets and stabilize them against further depolymerization, as has been demonstrated with microtubules in vitro (Panda et al., 1995).

Tubulin turnover restricted to plus end

The data show that tubulin is continuously added onto the ends of flagella that are not growing, implying that tubulin is turning over at steady state. But from which end of the flagellum are tubulin subunits removed? Either (a) addition and removal could both occur at the plus end (Fig. 4 A), or (b) tubulin could assemble at the plus end and disassemble from the minus end (treadmilling) (Fig. 4 B). Of the two mechanisms, treadmilling seems less likely a priori because outer doublet microtubules are continuous with the basal bodies, so it is unclear where or how subunit removal could take place by this process.

Regardless, we distinguished between these mechanisms using the strategy illustrated in Fig. 4 C. Unlabeled cells were deflagellated and allowed to regenerate flagella in the presence of cycloheximide. Under these conditions, flagella regenerate to half normal length because the pool of axonemal proteins is depleted (Rosenbaum et al., 1969; Johnson and Rosenbaum, 1992). These cells were mated with cells expressing HA-tubulin that had not been deflagellated, and hence still contained a full pool of axonemal precursor proteins. After mating, the extra protein pool donated by the HA-tagged cells allowed the half-length flagella to grow rapidly to the same length as the other two flagella (Johnson and Rosenbaum, 1992). Once all four flagella were of equal length, the experiment proceeded exactly as in Fig. 1, except that now the two flagella of the cell that regenerated its flagella in the presence of cycloheximide started out labeled over half their length.

If turnover occurs entirely at the plus end, newly incorporated, labeled tubulin would simply replace tubulin subunits that were already labeled, and would not affect unlabeled tubulin in the proximal half of the flagellum; thus, the unlabeled segment would maintain a constant length. In contrast, if turnover involved treadmilling, the unlabeled

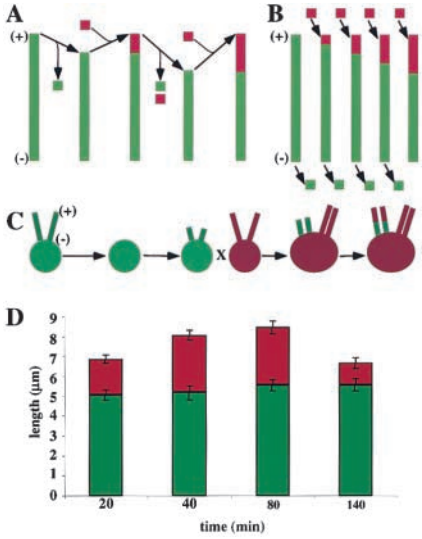

Figure 4. **Mechanism of flagellar microtubule turnover: plus end turnover versus treadmilling.** (A) Plus end only turnover model. Individual outer doublet microtubules alternate between cycles of growth and shortening, with all dynamics restricted to the plus end. Plus and minus ends of flagellar doublets are indicated by (+) and (−). (B) Treadmilling model. New subunits are assembled at the plus end of the outer doublets, while simultaneously, subunits are disassembled from the minus end. (C) Experimental strategy to distinguish plus end turnover from treadmilling. Cells with regenerated half-length flagella were mated to cells expressing HA-tubulin. Right after mating, the half-length flagella rapidly elongate to full length, incorporating HA-tubulin along their distal half. (D) Result of partial regeneration experiment. The unlabeled proximal segment did not shorten, either during the rapid regeneration phase or during the subsequent steady-state phase. This result is inconsistent with a treadmilling mechanism, but matches the predictions of the plus end turnover model. Average number of flagella measured per time point was 10.

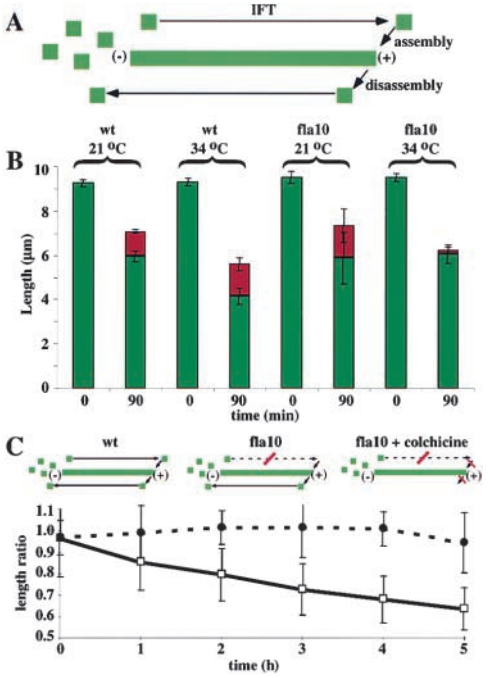

Figure 5. **Role of IFT in flagellar maintenance.** (A) Model: IFT particles carry structural proteins, including tubulin, to the plus end of the flagellum where they are incorporated in order to compensate for subunits removed during the disassembly portion of the turnover process. Plus and minus ends of the flagellar outer doublet microtubules are indicated by (+) and (−). (B) *fla10* mutants at the nonpermissive temperature block the assembly portion of turnover, as judged by the lack of tagged tubulin incorporation at the tip, but do not block disassembly, as judged by shortening of the unlabeled region of the flagella. This confirms that IFT is needed for ongoing incorporation of new tubulin at the distal end. Average number of measurements per graph entry was 19. (C) Colchicine is predicted to rescue the *fla10* phenotype by blocking outer doublet disassembly. As shown in graph, colchicine blocks flagellar resorption in *fla10* cells shifted to the nonpermissive temperature. (Dotted line) *fla10* cells treated with 3 mg/ml colchicine. (Solid line) Untreated *fla10* cells. Length ratio plots ratio of length at nonpermissive temperature to length at permissive temperature.

proximal segment should shorten because tubulin is constantly removed from the base of the flagellum.

As illustrated in Fig. 4 D, the results of this experiment are inconsistent with treadmilling: the unlabeled proximal segment did not shorten, either during the regeneration phase (which was completed within the first 20 min) or during the subsequent steady state phase that occurred once the flagella reached full length. Statistical analysis shows that slight differences in the unlabeled segment length at these time points are not significant. Even after 140 min, when the flagella have begun to shorten, the unlabeled segment length does not change, suggesting that not only assembly, but also disassembly, is restricted to the plus end. We conclude that the labeling of outer doublet microtubules seen in Fig. 1 occurs strictly by plus end turnover.

Intraflagellar transport balances plus end turnover

The continuous turnover of tubulin suggests that IFT is required to support the constant assembly at the distal end of the flagellum (Fig. 5 A). Presumably, if IFT is stopped, disassembly will continue and lead to flagellar resorption.

To test the model that IFT is required to support continuous tubulin assembly at the distal end in order to balance continuous tubulin removal, we measured tubulin incorporation in flagella of cells in which IFT has been stopped by the temperature-sensitive *fla10* mutation. The *fla10* mutation is known to cause a reduction in both the number and velocity (Kozminski et al., 1995; Iomini et al., 2001) of IFT particles in flagella at elevated temperatures. As seen in Fig. 5 B, wild-type cells and *fla10* mutant cells at the permissive temperature show similar levels of new tubulin incorporation, as judged by growth of the distal labeled flagellar segment, and they show similar levels of tubulin disassembly, as judged by shortening of the proximal unlabeled segment. In contrast, *fla10* mutant cells at the nonpermissive temperature showed almost no new tubulin incorporation (as judged by the almost complete lack of a distal labeled segment after 90 min), but showed the same rate of disassembly (as judged by shortening of the unlabeled proximal segment) as seen at the permissive temperature. Thus, IFT is needed to support the ongoing assembly of new tubulin at the distal ends of the outer doublets. We note that wild- type cells at 34°C appear to show a greater net loss of unlabeled tubulin compared with *fla10* cells at the same temperature, as judged by apparent shortening of the unlabeled proximal region. Our data do not suggest an obvious explanation for this interesting re-

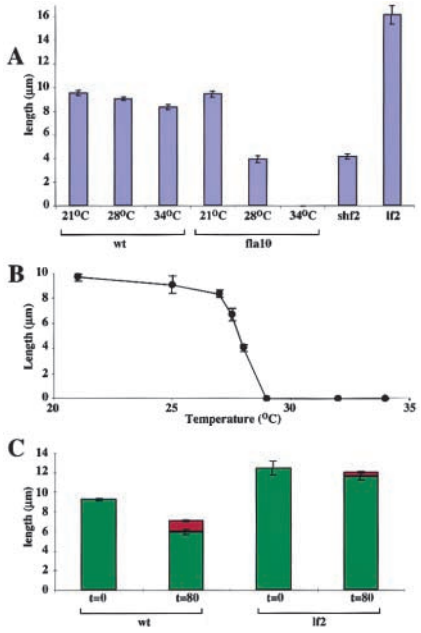

Figure 6. **Relationship between IFT, microtubule turnover, and flagellar length.** (A) Partial reduction of IFT causes *shf* phenotype. Bars depict length of flagella in wild-type and *fla10* cells grown at different temperatures. Typical *shf* and *lf* mutants are shown for comparison. In contrast to wild-type cells that show only a slight change in length at elevated temperatures, or temperature-sensitive *fla10* cells grown at the nonpermissive temperature in which flagella are completely resorbed, when *fla10* cells are grown at an intermediate temperature to partially reduce IFT, their flagella reach half length, comparable to bona fide *shf* mutants. (B) Length versus temperature in *fla10* mutant cells grown at a range of temperatures spanning completely permissive and completely nonpermissive, resulting in intermediate steady state length. Average number of measurements per data point is 25. (C) Reduction in microtubule turnover rate in *lf* mutant. Compared to wild-type cells measured over an equal time interval, *lf* mutant *lf2-5* shows less incorporation of new tubulin (reflected by the shorter length of incorporated tubulin at the plus end, indicated in red), as well as less removal of unlabeled tubulin (reflected by a smaller reduction in the length of the unlabeled proximal segment, indicated in green). Average number of measurements per entry in graph was 23.

sult. This may potentially reflect a coupling of assembly and disassembly at the plus end; however, this coupling cannot be absolute because the unlabeled region does in fact shorten in *fla10* cells, albeit not as rapidly as in wild-type cells.

To further investigate the relation between IFT and turnover, we noted that although colchicine has no effect on IFT itself (Kozminski et al., 1993b), it does block flagellar microtubule turnover (Fig. 3), raising the counterintuitive prediction that colchicine should block flagellar shortening in *fla10* mutants at the restrictive temperature. As shown in Fig. 5 C, this was indeed the case. Treatment of *fla10*-1 cells with colchicine blocked flagellar shortening following a shift to the nonpermissive temperature. This result further supports the model that flagella shorten in *fla10* mutants because IFT is normally required to balance flagellar disassembly during turnover.

Microtubule turnover and flagellar length mutants

The results of Fig. 5 suggest that intraflagellar transport is required continuously to maintain full-length flagella. This raises the possibility that if IFT were to be partially reduced, but not completely eliminated, it might cause a partial, but not complete, reduction in flagellar length. *fla10*^{ts} mutants were grown at an intermediate temperature between the fully permissive temperature of 21°C and the fully nonpermissive temperature of 34°C, so that some partial *fla10* function would remain. We found that in *fla10* cells grown at 28°C, the flagella shortened and equilibrated at roughly one half their wildtype length (Fig. 6 A), comparable to the lengths seen in previously identified *shf* mutants that can range in size from 5 to 8 μm, depending on the particular *shf* allele (Kuchka and Jarvik, 1987). This new length was maintained even after 3 d of growth at the intermediate temperature. Half-length flagella were only obtained when *fla10* cells were grown at exactly 28°C. Growing cells at a range of intermediate temperatures between fully permissive and fully nonpermissive produces a corresponding range of intermediate steady-state lengths (Fig. 6 B). When the temperature is increased to 29°C or higher, the flagella disappear completely, confirming that IFT in *Chlamydomonas* is strictly required to maintain even very short flagella.

If IFT maintains flagellar length by balancing turnover of microtubules at the plus end, then just as alterations in IFT can lead to changes in flagellar length, alterations in turnover rates should also lead to changes in flagellar length. Thus, some of the known *Chlamydomonas* flagellar length mutants (McVittie, 1972; Jarvik et al., 1976, 1984; Barsel et al., 1988; Kuchka and Jarvik, 1987; Asleson and Lefebvre, 1998) might show changes in outer doublet microtubule turnover rate. We tested this possibility by analyzing microtubule turnover in the *lf* mutant *lf2-5* (Barsel et al., 1988). As shown in Fig. 6 C, when the turnover assay was carried out in cells carrying the *lf2-5* mutation, the extent of turnover was greatly reduced compared with wild-type cells as reflected in a decrease in the growth of the labeled region (reflecting net assembly of labeled tubulin), as well as a decrease in the shortening of the unlabeled segment (reflecting net disassembly of unlabeled tubulin). This suggests that *lf2-5* may have *lf* because of a decrease in the disassembly rate.

IFT particles and flagellar length

Because IFT appears to play an important role in maintaining flagellar length, it is of interest to determine how the density of IFT particles may change as a function of flagellar length. Fig. 7 A shows three cells from a flagellar regeneration time course, stained with an antibody that detects the IFT protein IFT52 (Cole et al., 1998; Deane et al., 2001). Shorter flagella clearly show a more intense staining of IFT52 protein than longer flagella. Because it can be difficult to assess differences in fluorescence intensity by visual inspection, the average fluorescence intensity per unit length was quantified in cells at various stages of flagellar regeneration, and plotted in Fig. 7 B. This quantification confirms the visual impression that IFT52 is present at a higher concentration per unit length in shorter flagella, and becomes relatively less intense as the flagella become longer. Fig. 7 C plots the total IFT52 intensity in the flagellum, calculated by multiplying the intensity per unit length by the total length. This data indicates that the total amount of IFT52 in the flagellum is constant and does not vary significantly

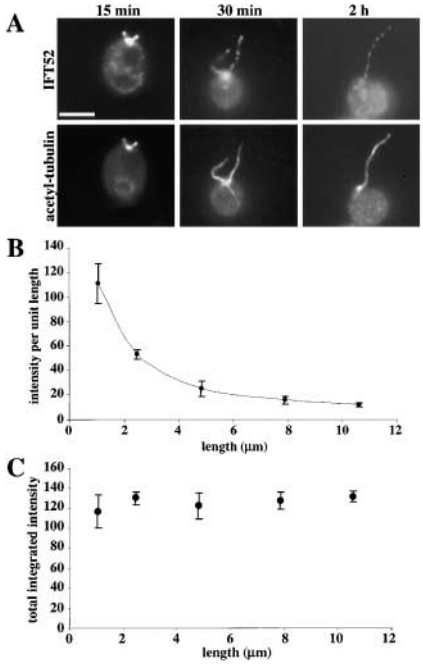

Figure 7. **Total quantity of intraflagellar transport particles is independent of flagellar length.** (A) IFT52 immunofluorescence staining during flagellar regeneration. Three cells are shown at three different time points during regeneration. As regeneration progresses and flagella elongate, the density of IFT52 decreases visibly. Bar, 5 μm. (B) Average IFT52 staining intensity, per unit length, plotted versus flagellar length. Quantification by digital imaging confirms the visual impression that IFT particle staining is more intense in short flagella. (C) Total IFT52 fluorescence intensity, a measure of IFT particle protein content, found by multiplying intensity per unit length by flagellar length. Graph indicates that the IFT particle content of a flagellum is independent of flagellar length.

with flagellar length. This result suggests that from the beginning of flagellar assembly, each flagellum is allocated a fixed number of active IFT particles, regardless of flagellar length. The consequences of this result for the mechanism of length control will be discussed below.

Discussion

A function of IFT in flagellar maintenance

IFT is required for flagellar and ciliary assembly and maintenance in a wide range of species (Rosenbaum et al., 1999). Given that flagellar assembly always takes place at the distal end of growing flagella (Johnson and Rosenbaum, 1992), the need for IFT during assembly is clear. However, the continued need for IFT to maintain flagella after flagellar growth has been completed has never been explained. If, as is often assumed, cilia and flagella are static structures, then it is hard to understand why IFT would be needed after flagellar assembly is completed. In this case, one would have to propose that IFT plays some additional function besides simply bringing flagellar proteins out to the distal tip assembly site. But the fact that flagellar proteins turn over (Stephens, 1997, 2000), together with the results presented here, that flagella are constantly removing and incorporating tubulin subunits at the distal ends of the outer doublets, leads to a much simpler explanation for the continuous requirement for IFT.

Because flagellar microtubules are constantly turning over, transport of fresh subunits is needed to support continuous assembly at the distal end. We have shown that when IFT is shut down, thus inhibiting assembly (Fig. 5 B), disassembly continues unabated, causing the flagella to shorten. We have also found that when turnover is blocked (i.e., by colchicine treatment), IFT is no longer required to maintain the flagella (Fig. 5 C). Therefore, we conclude that the primary role of IFT in maintaining cilia and flagella is to balance the ongoing disassembly of outer doublet microtubules by providing a constant supply of new material to assemble at the distal end. However, it is important to note that at present, we do not know exactly how IFT acts to bring material to the flagellar tip. Whether the IFT particles directly bind precursor proteins or instead facilitate their motion more indirectly, remains an open question that our data do not address.

Although shutting off IFT in *Chlamydomonas* by the *fla10* mutation results in complete loss of flagella at the nonpermissive temperature, antibody injection experiments in sea urchin embryos (Morris and Scholey, 1997) found that inhibiting kinesin-II (the homologue of *fla10*) resulted in short, paralyzed, but still visible cilia. This could either reflect a difference between sea urchins and *Chlamydomonas*, or differences in efficacy between antibody blocking approaches and direct mutations in the kinesin itself.

We also note that whereas this model accounts for the resorption of flagella when IFT is shut off, this may not be the only mechanism for resorbing a flagellum. In *Chlamydomonas*, recently mated cells retain their flagella for ~2 h and then rapidly resorb them prior to meiosis. This resorption is completed within just 20 min, and is thus much faster than the flagellar resorption seen when IFT is shut down, which takes several hours before resorbtion is complete. Moreover, whereas colchicine blocks the slow resorption of flagella in *fla10* mutants (Fig. 5 C) by arresting turnover, it has no effect on the rapid premeiotic flagellar resorption during mating (unpublished data). These differences suggest that the two types of resorption may occur via different mechanisms.

A model for flagellar length control

The preceding results yield three main facts that, taken together, suggest a simple model for flagellar length control: (a) flagellar microtubules turn over continuously at the plus end; (b) IFT is required for assembly at the plus end and must, therefore, be able to provide flagellar precursor proteins fast enough to balance the ongoing disassembly; and (c) the number of IFT particle proteins per flagellum is independent of flagellar length. We propose that flagellar length may be determined by an equilibrium between assembly and disassembly at the plus end.

In order to see how such an equilibrium can yield a unique steady-state length, we must consider the length dependence of the assembly and disassembly rates. When IFT is blocked in *fla10* mutants, flagella shorten at a constant rate, indicating that the disassembly rate at the plus end is independent of flagellar length. In contrast, when flagella regenerate, the rate of flagellar elongation decreases as the flagellum grows (Rosenbaum and Child, 1967; Tamm, 1967), indicating that the assembly rate is length dependent and decreases as the flagellum becomes longer.

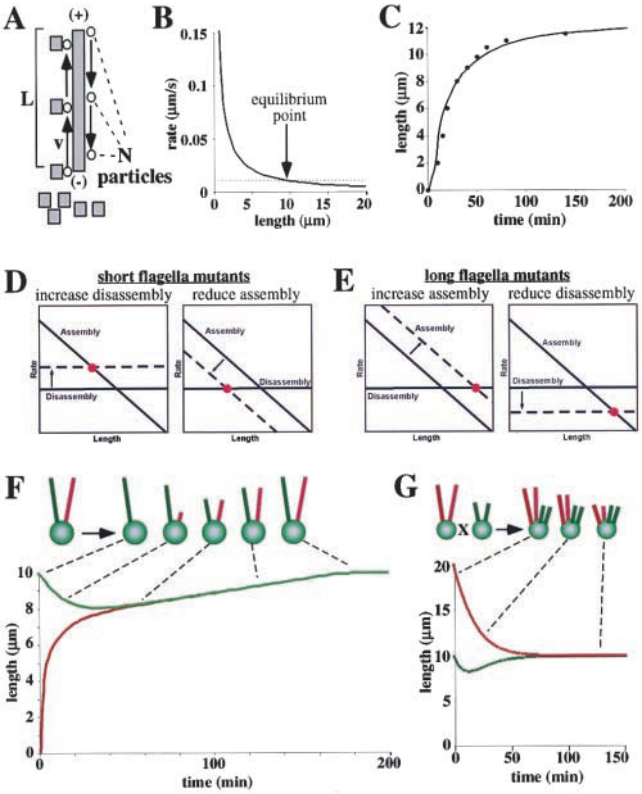

Figure 8. **Theoretical model for flagellar length control based on IFT and microtubule turnover.** (A) IFT leads to length-dependent assembly rate. Equation gives assembly versus length assuming that transport is rate limiting. N number of IFT particles cycling per flagellum. α, Constant reflecting the transport capacity of a single IFT particle; v, average velocity of an IFT particle; L, flagellar length. Squares represent flagellar precursor protein, for example tubulin. Circles represent IFT particles. (B) Length-dependent assembly predicted by IFT-limited transport leads to a steady-state mechanism for length regulation. (Solid line) Length-dependent assembly rate. (Dotted line) Length-independent disassembly rate. The flagellar length is the equilibrium length (arrow) at which the two rates balance. (C) Predicted kinetics of flagellar regeneration based on equation 1. (●) Data points taken from regeneration measurements in Rosenbaum et al. (1969). (Solid line) Best fit predicted regeneration kinetics. (D) Two possible causes of *shf* mutants. Either increasing disassembly rate (left) or decreasing assembly rate (right) will lead to equilibration at a shorter length. Thus, reduction in IFT is predicted to cause an *shf* phenotype, which accounts for the results of Fig. 6 A. (Solid line) Wild-type rates; (dotted line) rate in mutant cells; (●) new equilibrium point in mutant. (E) Two possible causes of *lf* mutants. Either increasing assembly rate (left) or decreasing disassembly rate (right) will lead to equilibration at a longer length. The ability of reduced turnover to cause *lf* phenotype accounts for the results of Fig. 6 C. (F) Turnover model predicts results of experiment in which a single flagellum is severed. Cartoon illustrates observed behavior of such cells: as the severed flagellum regenerates, the intact flagellum shortens until both reach the same length. Graph shows result of computer simulation based on length control model. (Red) Length of severed flagellum; (green) length of the unsevered flagellum. Dashed lines connect corresponding time points of simulated response with stages of observed response. (G) Simulation of experiments in which recessive *lf* mutants are fused with wild-type cells. (Red) *lf* shorten to wild-type length once the recessive mutation is complemented by wild-type cytoplasm; (green) wild-type flagella fluctuate in length, but eventually regain their normal length.

This length-dependent assembly follows from the mechanism of IFT (Fig. 8 A). If transport of flagellar components by IFT is the rate-limiting step in assembly, then the assembly rate should be proportional to $\alpha vN/2L$ where N is the number of IFT particles, L is the flagellar length, v is the average velocity of each IFT particle, and α is a constant reflecting the quantity of flagellar precursor protein transported per IFT complex (see Appendix for derivation). This expression is based on the data of Fig. 7 C, which shows that the number N of active IFT particles moving within the flagella is independent of flagellar length.

Combining length-dependent assembly with length-independent disassembly results in the situation illustrated in Fig. 8 B, in which the two rates will balance only at one unique length. In formal terms, we can combine the length-dependent assembly rate $\alpha vN/2L$ with a length-independent disassembly rate D to find the net rate of growth or shortening as a function of length, as follows:

$$dL/dt = avN/2L - D. \quad (1)$$

We find the steady-state solution by setting dL/dt equal to zero (corresponding to the intersection of the two curves in Fig. 8 B), showing that a stable length can only be maintained when $\alpha vN/2L = D$, which for a given set of values of α, v, N, and D, will only hold for a single value of L. If L were to somehow increase beyond this equilibrium value, the first term would become less than D, dL/dt would become negative, and the flagellum would shorten. Conversely, if the flagellum were too short, for example during regeneration, dL/dt would be positive, resulting in continued growth. Thus, the intrinsic length dependence of IFT-mediated tip assembly, combined with the length-independent tip disassembly inferred from resorption kinetics (Tamm, 1967), provides a simple and robust mechanism for length determination.

The simplified model described here involves the assumption that the disassembly rate D is a constant that is independent of length and assembly rates. However, neither of these assumptions is strictly required. As long as the disassembly versus length curve intersects the assembly versus length curve at a single point, the model will produce a unique stable flagellar length. Thus, it is not necessary for the disassembly rate to be completely independent of length or assembly rate, although it simplifies the mathematical form of the model.

In addition to providing a simple mechanism for maintaining length, the mathematical model of Eq. 1 can also account for the observed kinetics of flagellar regeneration. As illustrated in Fig. 8 C, the solution of Eq. 1 fits the observed regeneration kinetics data (Rosenbaum et al., 1969) almost exactly (see Appendix for details).

This model also makes specific predictions about flagellar length mutants. There are two ways to obtain an *shf* phenotype (Fig. 8 D). One is to increase the disassembly rate. In this case the two curves will intersect at a shorter equilibrium length, leading to an *shf* phenotype. Alternatively, the assembly rate could be decreased, and again the two curves will intersect at a shorter length. This second scenario predicts that a partial reduction in IFT should lead to a *shf* phenotype, as confirmed in Fig. 6 A.

The model of Eq. 1 also makes predictions about the types of mutations that would cause an *lf* phenotype. As illustrated in Fig. 8 E, *lf* mutants could arise in either of two ways. One is for the assembly versus length curve to increase, for example by increasing the number of functional IFT particles. Alternatively, the disassembly rate could be reduced. In both cases, the assembly and disassembly rate curves would intersect at a longer length. In the latter case, the turnover should be decreased at steady state. This prediction was demonstrated experimentally in the case of one *lf* mutant, as illustrated in Fig. 6 C. Because *lf2-5* mutants show decreased microtubule turnover leading to a longer flagellum, we suggest that the *lf2* gene product may promote microtubule turnover in the flagellum, although this effect may be indirect.

We note that many *lf* mutants also show defects in the timing and rate of flagellar regeneration (Barsel et al., 1988). Moreover, certain double mutant combinations of *lf* mutations block flagellar assembly completely. These pleiotropic phenotypes suggest the *lf* genes might have other cellular functions besides flagellar length control. The fact that a mutation in a single gene can cause multiple phenotypes is in no way surprising. For example, many kinases are involved in more than one cellular pathway because they recognize more than one substrate. If, as has been suggested, one or more *lf* genes encode kinases that regulate flagellar length (S. Berman, N. Haas, C. Asleson, and P. Lefebvre. 2000. Ninth International Conference on Cell and Molecular Biology of *Chlamydomonas*. 161 (Abstr.); Wilson and Lefebvre, 1999), then unless one proposes that such kinases can recognize only a single substrate, we should in fact expect mutations in such genes to have multiple phenotypes. When the *lf* genes are cloned and sequenced this may shed some light on the pleiotropic phenotypes of these mutations.

One interesting feature of flagellar length control is the fact that the flagella within a given cell will always adjust themselves to attain equal lengths, even if one of the two is severed (Rosenbaum et al., 1969; Coyne and Rosenbaum, 1970; Barsel et al., 1988). To see whether our length control model can account for this observation, we explored the behavior predicted by the model of Eq. 1 in cells with flagella of different lengths, by modifying the equation to include the assumption that the assembly rate, in addition to being length dependent, is also proportional to the size of the available precursor pool, as expected if IFT particles are in binding equilibrium with free axonemal subunits in the cytoplasm (see Appendix for details of the mathematical model and the resulting computer simulations). We then explored the predicted behavior for cells whose flagellar length become unequal, either by severing one flagellum or by mating *lf* mutants to wild-type cells.

First, we considered the case of severing one flagellum. When one flagellum on a biflagellate *Chlamydomonas* cell is severed while the other remains intact, the severed flagellum immediately begins to regenerate. At the same time, the other, initially intact, flagellum starts to shorten, and continues to do so, as the regenerating flagellum grows, until both reach the same length. In most cases, the shortening of the unsevered flagellum stops when the two flagella reach the same length, and then both flagella continue to grow out in parallel until they reach the final equilibrium length (Rosenbaum et al., 1969; Coyne and Rosenbaum, 1970). As illustrated in Fig. 8 F, computer simulations based on Eq. 1 (see Appendix for details) reproduce the essential features of this experiment. We note that in flagellar severing experiments, in some cases the shortening flagellum continued to shorten somewhat even after it had reached the same length as the regenerating flagellum, and our simple model does not predict this response. However, this type of behavior only occurred occasionally (Coyne and Rosenbaum, 1970). In any event, the most important feature of the flagellar severing experiments, i.e. the fact that the unsevered flagellum shortens in order to equalize length, is clearly explainable by the simple mechanism proposed here (Eq. 1).

Another example of flagellar length equalization occurs when recessive *lf* mutants are mated with wild-type cells. In the resulting quadriflagellate cells, the *lf* rapidly shorten until they reach the same length as the wild-type flagella (Barsel et al., 1988). However, as shown in Fig. 8 G, the length-regulation model of Eq. 1 is able to recapitulate this behavior in computer simulations (see Appendix for details of simulation).

Thus, the simple model presented here can account for both *shf* and *lf* mutants (Fig. 8, D–E), as well as the ability of flagella to equalize their lengths (Fig. 8, F and G). We conclude that it is not necessary to invoke a length sensor to account for many aspects of flagellar length control, which can instead by explained by a simple equilibrium between length-dependent IFT and outer doublet turnover.

One phenomenon of length control that is not directly addressed by our model is the fact that cells can modify the lengths of their flagella under some circumstances. For example *Chlamydomonas,* like many flagellated cells, resorb their flagella prior to cell division and then reassemble them after division. Recent work has revealed some evidence for a signal transduction cascade that regulates flagellar length in *Chlamydomonas* (Wilson and Lefebvre, 1999). The lack of a length sensor in the model presented here is by no means inconsistent with the existence of a pathway to modify flagellar length. Quite to the contrary, the model makes concrete predictions about possible control points for adjusting length. Perhaps the most obvious would be in controlling IFT itself. Signaling pathways converging on the IFT machinery could modulate the number of active IFT particles in the flagellum, thereby adjusting the assembly versus length curve, leading to stable changes in flagellar length. For example kinesin-II, the motor that drives anterograde IFT, may be subject to regulation via specific phosphorylation events (Reese and Haimo, 2000). IFT need not be the only target for a length modification pathway. Any changes to either the assembly or disassembly rate, such as modifications in the intrinsic stability of the outer doublet microtubules, is expected to result in changes in the steady state length. Thus, the present model provides a conceptual framework, not only for how flagellar length is set, but also for how it can be changed.

Materials and methods

Strains

Wild-type strain 6145c mt− selected for high mating efficiency and strong negative phototaxis was provided by Nedra Wilson (University of Minnesota, St. Paul, MN) The strain 5C12G12 mt+ expressing HA epitope–tagged α-tubulin was previously described (Kozminski et al., 1993a). The total level of α-tubulin in this strain is the same as in wild-type cells, and expression of the HA-tubulin has no effect on cell growth rate, cytoskeletal

morphology, tubulin acetylation, colchicine sensitivity, flagellar length, swimming rate, flagellar regeneration kinetics, or low calcium–induced flagellar resorbtion kinetics (Kozminski et al., 1993a). Therefore, we conclude that expression of this construct does not perturb flagellar microtubule dynamics.

Fla10-1 mt− mutant strain cc-1919 and *lf2-5* mt− mutant strain cc-2287 were obtained from the *Chlamydomonas* Genetics Center (Duke University, Durham, NC). Strains expressing HA-tubulin in *fla10* and *lf2* mutant backgrounds were constructed by crossing 5C12G12 with cc-1919 or -2287, and selecting tetrad products (Harris, 1989) that showed the mutant phenotype and that expressed tagged tubulin as judged by immunofluorescence.

Mating procedure

Gamete cultures of 5C12G12 mt+ and 6145c mt− were obtained using standard methods (Harris, 1989). 500 μL of each culture was then mixed together and allowed to mate for 15 min. To arrest mating, 5 ml of low nitrogen medium (Harris, 1989) was added to the mating mixture, which was then allowed to sit undisturbed for 15 min. During this time, the negatively phototactic mt− cells swam to the bottom of the tube to form a pellet, along with the majority of the quadriflagellated dikaryons, which become negatively phototactic after mating. The mt+ cells, which were nonphototactic under these conditions, remained in suspension. The top 4 mL of medium was removed and replaced with 4 mL fresh medium. This procedure was repeated twice more to remove unmated mt+ cells, thereby arresting further mating. The remaining cells were diluted to a total volume of 10 mL to further discourage additional mating.

Immunofluorescence

Immunofluorescence was performed as described (Cole et al., 1998). Primary antibodies were mouse monoclonal anti-HA antibody 12CA5 diluted 1:10, and affinity-purified rabbit anti-*Fla10* (Cole et al., 1998) diluted 1:250. Affinity-purified rabbit anti-IFT52 antibodies were provided by James Deane (Deakin University, Melbourne, Austrailia) and diluted 1:50. Secondary antibodies were Oregon green goat anti–rabbit (Molecular Probes) plus Texas red goat anti–mouse (Jackson ImmunoResearch Laboratories), each diluted 1:500. We note that when *Chlamydomonas* cells adhere to polylysine-coated coverslips for long periods of time, the tips of the flagella begin to curl up, such that even antibodies that stain the flagellum uniformly along its length sometimes give a brighter signal at the tip. Therefore, we minimized the time (always <5 min) that the cells were allowed to adhere to the coverslips. Cells fixed immediately after mating showed no tip labeling, indicating that the tip labeling observed in Fig. 1 was not simply an artifact due to tip curling.

For distinguishing central pair from outer doublet microtubules, flagella on intact cells were de-membranated and splayed using NP-40 plus ATP as previously described (Johnson, 1998). The partial regeneration experiment of Fig. 4 was performed as described (Johnson and Rosenbaum, 1992). Slides were imaged with a 63× NA1.4 oil immersion objective. Lengths were measured using a calibrated reticule mounted in the ocular.

For imaging IFT52 staining versus flagellar length, wild-type cells were deflagellated by pH shock. Cells were stained with antibodies to IFT52 and acetylated tubulin, and imaged using a cooled CCD using a uniform exposure time. Average intensity was measured in a series of 20 × 20 windows that spanned the length of the flagella.

Appendix

Mathematical model of flagellar length control

Derivation of differential equation describing length regulation. To obtain the differential equation describing flagellar tubulin turnover (Eq. 1), we assume that IFT-mediated precursor transport is the rate-limiting step that determines the addition rate of new tubulin subunits at the distal end. Direct measurements have shown that IFT particles move at a constant rate of $v_a = 2$ μm/s in the anterograde direction, and $v_r = 3.5$ μm/s in the retrograde direction (Kozminski et al., 1993b). The time it takes for a particle to move from the base to the tip and back again over a length L is given by 2L/v, where v is an effective velocity equal to $2v_av_r/(v_a + v_r)$ which, given the measured values for IFT, is equal to 2.5 μm/s. This simple model assumes that the number of particles moving anterograde equals the number moving retrograde, which may not be strictly true. However, the fundamental predictions of these simulations are not affected if one changes the relative ratio of anterograde to retrograde particles. If there are N transport complexes moving in a single flagellum, we obtain the expression αvN/2L as the assembly rate at the tip, where α is a proportionality constant reflecting the effective transport capacity of each IFT particle. We assume that disassembly occurs at a constant rate D, estimated to be 0.011 μm/s, based on the rate at which flagella resorb during the rapid disassembly period after mating (10 μm in 15 min). We can then solve for α by considering the steady-state situation where D = αvN/2L. We set N = 10 based on typical DIC images, but any other number would give the exact same results because we solve for α in terms of N. The plot of Fig. 8 B was obtained by computing the value of αvN/2L for different values of L.

Prediction of flagellar regeneration kinetics. The flagellar regeneration plot (Fig. 8 C) was produced by solving Eq. 1 to yield:

$$T = \{A - DL - A\ln|A - DL|\}/D^2 + C \qquad (A1)$$

where A = αvN/2, D is the disassembly rate, T is time, and C is a constant of integration. We fit Eq. A1 to a published time-course of flagellar regeneration (Rosenbaum et al., 1969). The solution plotted in Fig. 8 C corresponds to A = 2.67 μm2/min, D = 0.22 μm/min, and a lag before initiation of regeneration (determined by letting the constant of integration C vary to obtain the optimal fit) of 3.0 min. The r.m.s. error in T was 7.4 min.

Simulation of flagellar severing experiments. To simulate experiments in which flagellar length reequalizes following perturbations such as severing one flagellum, it is necessary to model the effects of flagellar severing on the pool of flagellar precursor proteins. The simplest assumption is that axonemal proteins are loaded onto IFT particles according to a simple binding equilibrium so that the amount of material transported by each IFT particle is proportional to the available pool of flagellar precursor proteins.

Let *P* represent the total pool of flagellar precursor protein, including both free precursor and that already incorporated into flagella. Specifically, *P* refers to the quantity of whichever flagellar structural protein is limiting. At present it is not known whether this is tubulin or some other protein. We find *P* by noting that *Chlamydomonas* cells contain a free protein pool sufficient to build two half-length flagella without additional protein synthesis if both flagella are cut off (Rosenbaum et al., 1969). Therefore, the total pool size *P* is found by solving for steady state conditions, both for normal cells in which a complete pool gives two full-length flagella, and for deflagellated cells for which a pool reduced by two flagella worth of material yields two half-length flagella at steady state. For any given total pool size, the free pool of protein will be *P* minus the quantity of protein incorporated into the two flagella, or $P - L1 - L2$. Therefore, we replace the original rate coefficient α in Eq. 1 with a pool-dependent rate coefficient $\beta(P - L1 - L2)$ where β is a constant.

To simulate the severing of one flagellum, the length of the severed flagellum was set to 0.1 μm (to avoid division by zero) and the initial length of the unsevered flagellum was

set to 10 μm, the normal length of a *Chlamydomonas* flagellum. Therefore, the total pool size was decreased by the equivalent of one flagella worth of protein. The pool was modeled as regenerating at a rate sufficient to regenerate two flagella to half length in 30 min. To obtain the time course of flagellar length after severing (Fig. 8 F), the differential equations for the two flagella were integrated using the Euler method with a step size in time of 0.1 s.

Simulation of length equalization following fusion of wild-type and *lf* mutant cells. To simulate experiments in which recessive *lf* mutants are fused with wild-type cells to form dikaryons (Fig. 8 G), two flagella were set to an initial length of 20 μm and two were set to the wild-type length of 10 μm. α,v, N, and D, were set to the same values used for wild-type cells, assuming the recessive *lf* mutation is completely complemented after cell fusion.

Doug Cole and Dennis Diener were instrumental in designing the turnover visualization assay described here, and the authors gratefully acknowledge their contribution. We thank Nedra Wilson, Dennis Diener (Yale University, New Haven, CT), and the *Chlamydomonas* Genetics Center for strains, Doug Cole (University of Idaho, Moscow, ID) and James Deane for antibodies, Jennifer Fung for advice on digital imaging microscopy, and Nedra Wilson, Pete Lefebvre, and Michael Melkonian for helpful discussions. We also thank Diane Casey, Dennis Diener, Jennifer Fung, Eun-Jin Hong, Naomi Morrissette, Lotte Pedersen, Ray Stephens, and Hongmin Qin for careful reading of the manuscript.

This work was supported by National Institutes of Health grant GM14642 to J.L. Rosenbaum. W.F. Marshall was supported by a Helen Hay Whitney Foundation postdoctoral fellowship and a Leukemia and Lymphoma Society Special Fellowship.

Submitted: 26 June 2001
Revised: 23 August 2001
Accepted: 20 September 2001

References

Asleson, C.M., and P.A. Lefebvre. 1998. Genetic analysis of flagellar length control in *Chlamydomonas* reinhardtii: a new long-flagella locus and extragenic suppressor mutations. *Genetics.* 148:693–702.

Barsel, S.E., D.E. Wexler, and P.A. Lefebvre. 1988. Genetic analysis of long-flagella mutants of *Chlamydomonas* reinhardtii. *Genetics.* 118:637–648.

Behnke, O., and A. Forer. 1967. Evidence for four classes of microtubules in individual cells. *J. Cell Sci.* 2:169–192.

Cole, D.G., D.R. Diener, A.L. Himelblau, P.L. Beech, J.C. Fuster, and J.L. Rosenbaum. 1998. *Chlamydomonas* kinesin-II–dependent intraflagellar transport (IFT): IFT particles contain proteins required for ciliary assembly in *Caenorhabditis elegans* sensory cilia. *J. Cell Biol.* 141:993–1008.

Coyne, B., and J.L. Rosenbaum. 1970. Flagellar elongation and shortening in *Chlamydomonas*. II. Reutilization of flagellar proteins. *J. Cell Biol.* 47:777–781.

Deane, J.A., D.G. Cole, E.S. Seely, D.R. Deiner, and J.L. Rosenbaum. 2001. Localization of the intraflagellar transport protein IFT52 identifies the transitional fibers of the basal bodies as the docking site for IFT particles. *Curr. Biol.* In press.

Fujiwara, M., T. Ishihara, and I. Katsura. 1999. A novel WD40 protein, CHE-2, acts cell-autonomously in the formation of *C. elegans* sensory cilia. *Development.* 126:4839–4848.

Gorovsky, M.A., K. Carlson, and J.L. Rosenbaum. 1970. Simple method for quantitative densitometry of polyacrylamide gels using fast green. *Anal. Biochem.* 35:359–370.

Harris, E.H. 1989. The *Chlamydomonas* Sourcebook. Academic Press, San Diego, CA. 780 pp.

Huang, B., M.R. Rifkin, and D.J. Luck. 1977. Temperature-sensitive mutations affecting flagellar assembly and function in *Chlamydomonas* reinhardtii. *J. Cell Biol.* 72:67–85.

Iomini, C., V. Babaev-Khaimov, M. Sassaroli, and G. Piperno. 2001. Protein particles in *Chlamydomonas* flagella undergo a transport cycle consisting of four phases. *J. Cell Biol.* 153:13–24.

Jarvik, J., P.A. Lefebvre, and J.L. Rosenbaum. 1976. A cold-sensitive mutant of *Chlamydomonas* reinhardtii with aberrant control of flagellar length. *J. Cell Biol.* 70:149a.

Jarvik, J.W., F.D. Reinhardt, M.R. Kuchka, and S.A. Adler. 1984. Altered flagellar size control in *shf-1* short flagellar mutants of *Chlamydomonas* reinhardtii. *J. Protozool.* 31:100–104.

Jensen, C.G., E.A. Davidson, S.S. Bowser, and C.L. Rieder. 1987. Primary cilia cycle in PtK1 cells: effects of colcemid and taxol on cilia formation and resorption. *Cell Motil. Cytoskeleton.* 7:187–197.

Johnson, K.A. 1998. The axonemal microtubules of the *Chlamydomonas* flagellum differ in tubulin isoform content. *J. Cell Sci.* 111:313–320.

Johnson, K.A., and J.L. Rosenbaum. 1992. Polarity of flagellar assembly in. *Chlamydomonas. J. Cell Biol.* 119:1605–1611.

Kozminski, K.G., D.R. Diener, and J.L. Rosenbaum. 1993a. High level expression of nonacetylatable α-tubulin in *Chlamydomonas* reinhardtii. *Cell Motil. Cytoskeleton.* 25:158–170.

Kozminski, K.G., K.A. Johnson, P. Forscher, and J.L. Rosenbaum. 1993b. A motility in the eukaryotic flagellum unrelated to flagellar beating. *Proc. Natl. Acad. Sci. USA.* 90:5519–5523.

Kozminski, K.G., P.L. Beech, and J.L. Rosenbaum. 1995. The *Chlamydomonas* kinesin-like protein *FLA10* is involved in motility associated with the flagellar membrane. *J. Cell Biol.* 131:1517–1527.

Kuchka, M.R., and J.W. Jarvik. 1987. Short-flagella mutants of *Chlamydomonas*. *Genetics.* 115:685–691.

McVittie, A.C. 1972. Flagellum mutants of *Chlamydomonas reinhardtii*. *J. Gen. Microbiol.* 71:525–540.

Morris, R.L., and J.M. Scholey. 1997. Heterotrimeric kinesin-II is required for the assembly of motile 9+2 ciliary axonemes on sea urchin embryos. *J. Cell Biol.* 138:1009–1022.

Panda, D., J.E. Daijo, M.A. Jordan, and L. Wilson. 1995. Kinetic stabilization of microtubule dynamics at steady state in vitro by substoichiometric concentrations of tubulin-colchicine complex. *Biochemistry.* 34:9921–9929.

Piperno, G., K. Mead, and S. Henderson. 1996. Inner dynein arms, but not outer dynein arms, require the activity of kinesin homologue protein KHP1 (*FLA10*) to reach the distal part of flagella in *Chlamydomonas*. *J. Cell Biol.* 133:371–379.

Reese, E.L., and L.T. Haimo. 2000. Dynein, dynactin, and kinesin II's interaction with microtubules is regulated during bidirectional organelle transport. *J. Cell Biol.* 151:155–166.

Rosenbaum, J.L., and F. Child. 1967. Flagellar regeneration in protozoan flagellates. *J. Cell Biol.* 34:345–364.

Rosenbaum, J.L., J.E. Moulder, and D.L. Ringo. 1969. Flagellar elongation and shortening in *Chlamydomonas*. The use of cycloheximide and colchicine to study the synthesis and assembly of flagellar proteins. *J. Cell Biol.* 41:600–619.

Rosenbaum, J.L., D.G. Cole, and D.R. Diener. 1999. Intraflagellar transport: the eyes have it. *J. Cell Biol.* 144:385–388.

Song, L., and W.L. Dentler. 2001. Flagellar protein dynamics in *Chlamydomonas. J. Biol. Chem.* 276:29754–29763.

Stephens, R.E. 1992. Tubulin in sea urchin embryonic cilia: characterization of the membrane-periaxonemal matrix. *J. Cell Sci.* 100:521–531.

Stephens, R.E. 1997. Synthesis and turnover of embryonic sea urchin ciliary proteins during selective inhibition of tubulin synthesis and assembly. *Mol. Biol. Cell.* 8:2187–2198.

Stephens, R.E. 2000. Preferential incorporation of tubulin into the junctional region of ciliary outer doublet microtubules: a model for treadmilling by lattice dislocation. *Cell Motil. Cytoskeleton.* 47:130–140.

Tamm, S.L. 1967. Flagellar development in the protozoan *Paranema trichophorum*. *J. Exp. Zool.* 164:163–186.

Tilney, L.G., and J.R. Gibbins. 1968. Differential effects of antimitotic agents on the stability and behavior of cytoplasmic and ciliary microtubules. *Protoplasma.* 65:167–179.

Tilney, L.G., P.S. Connelly, K.A. Vranich, M.K. Shaw, and G.M. Guild. 2000. Actin filaments and microtubules play different roles during bristle elongation in *Drosophila*. *J. Cell Biol.* 113:1255–1265.

Wilson, N.F., and P.A. Lefebvre. 1999. Pharmacological analysis of the regulation of flagellar length in *Chlamydomonas*. *Mol. Biol. Cell.* 10:387a.